

Nitromethane Ignition Behind Reflected Shock Waves

O. Mathieu¹, B. Giri², J. D. Mertens, and E. L. Petersen¹

¹Texas A&M University, Department of Mechanical Engineering
College Station, Texas, USA

²Trinity College, Department of Engineering
Hartford, Connecticut, USA

1 Introduction

Due to its properties as a fuel component, there is a lot of interest around the detailed understanding of nitromethane's combustion chemistry. When blended with gasoline, nitromethane (NM) induces an increase in octane sensitivity (RON-MON) [1], which is beneficial to prevent knock in modern, direct-injected, boosted gasoline engines [2]. Nitromethane also has a high lubricity, which is interesting for model and racing engines [3]. Additionally, the relatively small size of NM with regards to its oxygen content allows the introduction of more fuels into the cylinder for a given quantity of air, leading to a higher energy output, useful for racing engines. Finally, NM is used as a reference component to understand the combustion mechanism of solid propellant [4] and is considered as a possible replacement for hydrazine as a monopropellant [5]. Despite these various interests, the combustion chemistry of NM has been investigated in only a few studies. Although the pyrolytic decomposition of NM has been largely covered over a few decades [6, 7], the thermal decomposition of NM has not been so well characterized in terms of reaction rates until the study of Glarborg et al. [8], where the reaction rate for two key reactions ($\text{CH}_3\text{NO}_2 (+\text{M}) \rightleftharpoons \text{CH}_3 + \text{NO}_2 (+\text{M})$ (R1) and $\text{CH}_3 + \text{NO}_2 \rightleftharpoons \text{CH}_3\text{O} + \text{NO}$ (R2)) were re-evaluated. The flame structure of NM was then investigated numerically by Boyer and Kuo [4] and flame species formed in a premixed flame in Ar were identified [9]. A comprehensive mechanism based on the work from Glarborg et al. [8] was developed [10], and this last mechanism was recently improved by Brequigny et al. [3] who also measured the laminar flame speed of NM at various ϕ , between 0.5 and 3 bar. One can also mention the ignition delay time (τ_{ign}) measurements by Kang et al. [11], where the pressure is not reported, making these data difficult to use to further validate models. To help improving predictions on NM's combustion, the aim of the present study was to measure τ_{ign} for NM over large ranges of temperature, pressure, dilution and equivalence ratio in a shock tube.

2 Experimental setup

Ignition delay times were measured using the chemiluminescence emission from the $\text{A}^2\Sigma^+ \rightarrow \text{X}^2\Pi$ transition of the excited-state hydroxyl radical (OH^*) in a stainless-steel shock tube. The driver section is 2.46 m long (76.2-mm i.d.), and the driven section is 4.72 m long (152.4-mm i.d.). Post reflected-shock conditions were obtained using the extrapolated incident shock wave speed in conjunction with

1D shock relations and the initial conditions in the test region. In the same plane as the last pressure transducer, a sapphire window is mounted so as to pass light from the combustion zone onto a photomultiplier tube (Hamamatsu 1P21) equipped with an interference filter (307 ± 25 nm). Test pressure was monitored by one PCB 134A transducer located at the endwall and one Kistler 603 B1 transducer located at the sidewall. Details and schematics of the shock-tube setup can be found in Aul et al. [12].

To limit the number of experiments and still investigate a wide range of conditions, a design of experiments (DOE) test matrix was developed. Three levels of each variable (pressure, ϕ , dilution level) were assembled into an L9 Taguchi array, a method used by the authors' group in the past [12]. Normally, a L9 array does not allow for a direct comparison of the data at a given condition. Nevertheless, since some extra conditions and mixtures were studied, it was possible to compare some mixtures based on criteria such as equivalence ratio, pressure or dilution level. These comparisons made possible the presentation and discussion of all the mixtures investigated during this study with a few figures only. However, probably because of the lack of data varying around a condition (pressure, equivalence ratio etc.) with the L9 matrix, it was not possible to derive with a satisfactory R^2 a multi-regression analysis equation describing all measured ignition delay times as function of pressure, temperature, equivalence ratio and dilution. Table 1 summarizes the conditions investigated during this study. Mixtures were prepared manometrically into a stainless-steel mixing tank equipped with a perforated stinger traversing its center to allow for rapid, turbulent mixing. Nitromethane was first evaporated to no more than 60% of its vapor pressure at room temperature. Mixtures were then allowed to rest for at least 2 hours. Due to the low vapor pressure of NM, it was not possible to reach the same P_5 for the high-pressure cases of all dilution levels (Mix7-9). It was also not always possible to prepare mixtures large enough in the mixing tank to fill up the shock tube at the required pressure. To overcome these limitations, the maximum possible pressure for each dilution case (considering the vapor pressure of NM) was investigated, and mixtures were prepared directly in the driver section whenever needed. Due to the absence of a mixing device in the shock tube, it was then necessary to leave the mixture to rest for at least 10 hours. Helium was mostly used as the driver gas, although N_2 addition was occasionally used to reduce the speed of the incident wave and reach lower temperatures without increasing the initial pressure into the test section.

Table 1: Mixture compositions and conditions investigated for the ignition delay time measurements.

Mixture	ϕ	CH_3NO_2 %	O_2 %	Ar %	Avg. P_5 (atm)	T_5 range (K)	Diaphragm thickness (mm)
1	0.5	4.0	6.0	90.0	2.1	920-1215	Lexan, 0.25 mm
2	1.0	2.857	2.0143	95.0	1.9	1215-1495	Lexan, 0.25 mm
3	2.0	1.455	0.545	98.0	1.8	1420-1595	Lexan, 0.25 mm
4	0.5	2.0	3.0	95.0	2.0	1080-1450	Lexan, 0.25 mm
					11.5	955-1210	Aluminum, 1.52 mm
5	1.0	1.143	0.857	98.0	1.9	1300-1575	Lexan, 0.25 mm
					10.4	1255-1485	Lexan, 0.25+0.5+1.02 mm
6	2.0	7.273	2.727	90.0	8.6	890-1010	Lexan, 0.25+1.02 mm
7	0.5	0.8	1.2	98.0	2.0	1215-1460	Lexan, 0.25 mm
					34.3	1185-1375	Aluminum, 2.29 mm
8	1.0	5.714	4.286	90.0	9.4	895-1055	Lexan, 0.5+1.02 mm
9	2.0	3.64	1.36	95.0	13.7	875-1080	Lexan, 2×1.02 mm
10	1.0	0.571	0.429	99.0	1.9	1340-1540	Lexan, 0.25 mm

3 Results

3.1. Determination method

Ignition delay time, or τ_{ign} , is defined as the time between the passage of the reflected shock wave, indicated by a pressure jump in the signal delivered by the pressure transducer, and the intersection of lines drawn along the steepest rate-of-change and zero-concentration level of the OH^* profile (see Fig. 1 (a) and (b)). Due to a very low and continuous increase in the slope of the ignition peak right after the first OH^* peak, τ_{ign} was measured at the peak of the OH^* signal for the Mix 7, high-pressure (35 atm) case. As visible in Fig. 1, the OH^* profile of NM varies significantly with the experimental conditions. These variations are presented and discussed later. The total uncertainty in τ_{ign} from all contributions is estimated to be below 20%.

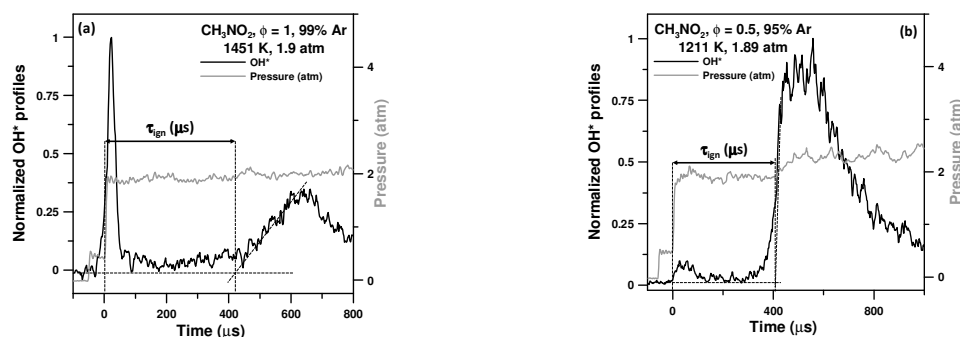


Figure 1: Typical sidewall experimental pressure and OH^* profiles and method of determination of the ignition delay time.

3.2. Experimental results

Equivalence ratio effect

The effect of ϕ on τ_{ign} is visible in Fig. 2(a) where results for mixtures in 98% Ar and at around 1.9 atm, are presented. As can be seen, increasing ϕ leads to an increase in τ_{ign} : at around 1420 K, τ_{ign} is increased by a factor >3 when ϕ is doubled, from 0.5 (135 μs) to 1.0 (450 μs). This increase in τ_{ign} reaches a factor >13 between the fuel lean and rich (1800 μs) cases. To illustrate the variations in the OH^* profiles with ϕ , normalized OH^* profiles are compared in Fig. 2 for (b) a similar temperature (1465 \pm 8 K) and (c) a similar τ_{ign} (445 \pm 12 μs). Profiles were normalized to the highest value reached, whether this value was reached on the 1st or the 2nd peak. For a given temperature (Fig. 2(b)), the 2nd peak corresponding to the ignition is the highest for the fuel lean case, whereas the highest OH^* amount is reached at the 1st peak for the $\phi = 1.0$ and 2.0 cases. One can also see that as ϕ increases, the intensity of the ignition peak decreases (but the peak becomes wider). For the case where a similar τ_{ign} was measured, Fig. 2(c), the maximum OH^* intensity is also reached on the 1st peak for the $\phi = 1.0$ and 2.0 conditions, while the maximum is reached at ignition for the $\phi = 0.5$ case (the intensity between the two peaks is close in this case). Again, the intensity of the ignition peak tends to decrease as ϕ increases, despite the fact that the temperature increases with ϕ for a given τ_{ign} (OH^* intensity typically increases with the temperature for a given mixture). One can therefore conclude from these observations that the intensity of the ignition peak rapidly decreases with the increase in ϕ .

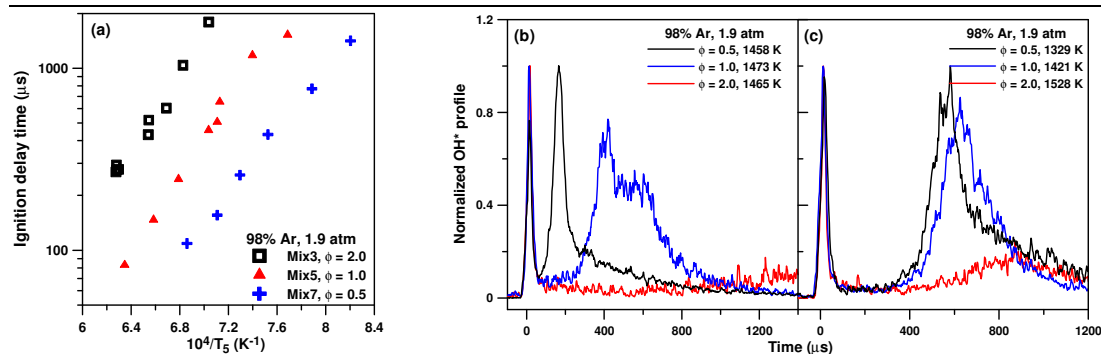


Figure 2: Effect of the equivalence ratio for mixtures diluted in 98% Ar and for P_5 around 1.9 atm.

Pressure (P_5) effect

The effect of P_5 on τ_{ign} is visible in Fig. 3 for (a) Mix 4, (b) Mix 5, and (c) Mix 7. For all cases, an increase in P_5 induces a decrease in τ_{ign} . However, the amplitude of this decrease is dependent on both ϕ and the dilution level. The influence of ϕ on the pressure effect can be observed by comparing results for Mix 5 and Mix 7. Both mixtures were diluted in 98% Ar, but when the P_5 is increased by a factor around 5 for Mix 5 ($\phi = 1.0$) (from around 1.9 atm to around 10.4 atm), τ_{ign} decreases by a factor between 2.3 (low temperature) to 1.6 (high temperature). For the Mix 7 case ($\phi = 0.5$), despite an increase in pressure by a factor of 17 (from around 2.0 to around 34.3 atm), τ_{ign} is decreased by smaller factors, from around 1.3 (high temperature) to around 1.7 (low temperature). Note that this smaller difference in τ_{ign} is partly due to the difference in the determination method of τ_{ign} .

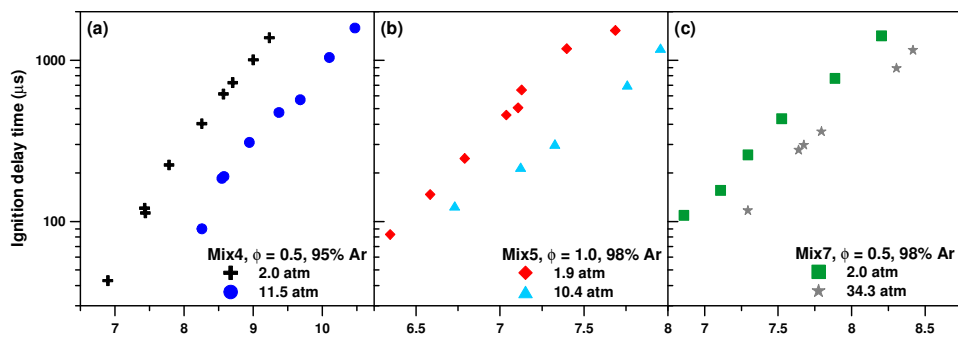


Figure 3: Effect of the pressure on the ignition delay time of NM.

The effect of P_5 on the OH^* profile was investigated as well, and it was found that OH^* profiles are somewhat similar for a given mixture, regardless of the pressure. It can be concluded that the pressure is not a very important factor regarding the intensity of one peak with regards to the other within the conditions investigated in this study.

Dilution level effect

The effect of the dilution level on τ_{ign} can be seen in Fig. 4(a)-(d). In nearly all conditions, the decrease in the dilution level leads to a decrease in τ_{ign} . In addition, this decrease depends on both the pressure and ϕ . For the low-pressure cases, Fig. 4 (a) and (b), the decrease in τ_{ign} is proportionally larger on the low-temperature side than on the high-temperature side. At $\phi = 0.5$ ((a)), decreasing the dilution level from 98% to 90% significantly reduces τ_{ign} at around 1220 K, from around 1400 μs for Mix 7 (98% Ar) to 400 μs and 75 μs for Mix 4 (95% Ar) and Mix 1 (90% Ar), respectively. Nevertheless, the difference between the mixtures diminishes as the temperature increases: τ_{ign} is around 2.5 times shorter for Mix 4 than for Mix 1 at 1450 K, against a factor of 3.5 at 1220 K. A similar observation can be made at $\phi = 1.0$ (Fig. 4(b)). As can be seen, τ_{ign} for the highly diluted mixtures (Mix 10, 99%

Ar) are even lower than for Mix 5 (98% Ar) above 1500 K. For the lowest temperature common to these three mixtures, 1340 K, τ_{ign} decreases from around 2050 μs (Mix 10, 99% Ar) to around 1215 μs (Mix 5, 98% Ar) and around 370 μs (Mix 2, 95% Ar). For the high-pressure case, Fig. 4(c) and (d), a very large difference is observed for the $\phi = 1.0$ data, between Mix 5 (98% Ar) and Mix 8 (90% Ar): the two sets of data do not share the same range of temperature within the observation time of the shock tube. On the other hand, data at fuel rich conditions (Fig. 4(d)) are very close to each other despite the change in dilution (90% Ar for Mix 6, 95% Ar for Mix 9). Note that this small difference can also be partly due to the difference in pressure between the two sets of data (8.6 atm for Mix 6 and 13.7 atm for Mix 9).

The dilution effect on the OH* profiles is visible in Fig. 5 for mixtures at $\phi = 0.5$ at around 2 atm for (a) a similar temperature (1215 ± 4 K) and (b) a similar τ_{ign} . As can be seen in Fig. 5(a), the highest intensity in the OH* signal is reached by the ignition peak for all dilutions investigated, between 98 and 90% Ar. However the intensity of the first peak varies greatly with the dilution level. The intensity of the first peak is less than 5% of the ignition peak for the 90% Ar case, and this ratio increases to 10% and 85% for the 95% and 98% Ar dilution, respectively. A similar trend is observed for the case where the profiles match a similar τ_{ign} (Fig. 5(b)). In that case, the first peak's intensity is around 4%, 25%, and 75% of the ignition peak for Ar concentration of 90%, 95%, and 98%, respectively. One can therefore conclude that the intensity of the ignition peak compared to the first peak increases with the Ar concentration.

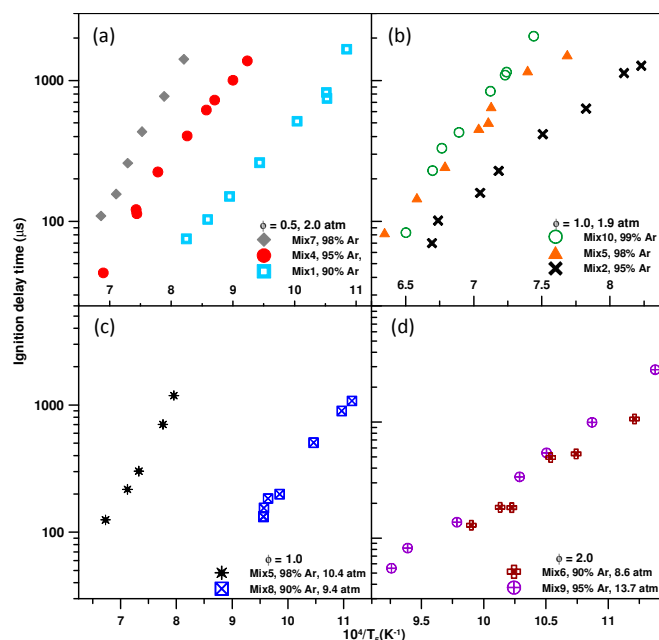


Figure 4: Effect of the dilution level in Ar on the ignition delay time of NM at around 2 atm for (a) $\phi = 0.5$, and (b) $\phi = 1.0$ and around 10 atm for (c) $\phi = 1.0$ and (d) $\phi = 2.0$.

4 Conclusions

Ignition delay times for nitromethane have been measured in a shock tube under conditions that have never been investigated heretofore. Wide ranges of conditions were investigated in terms of temperature (875-1595 K); pressure (1.8-34.3 atm); equivalence ratio (0.5, 1.0, and 2.0); and dilution (99, 98, 95, and 90% Ar) using an L9 Taguchi array. Results showed that nitromethane's ignition is very sensitive to most of these parameters. In addition, the OH* profile for nitromethane presents an interesting double feature, with the intensity between these two peaks varying greatly depending on the experimental conditions. Future work will include the development of a detailed kinetics

mechanism to reproduce these data as well as the literature data. This mechanism will also be interrogated to explain the double feature observed on the OH* profile.

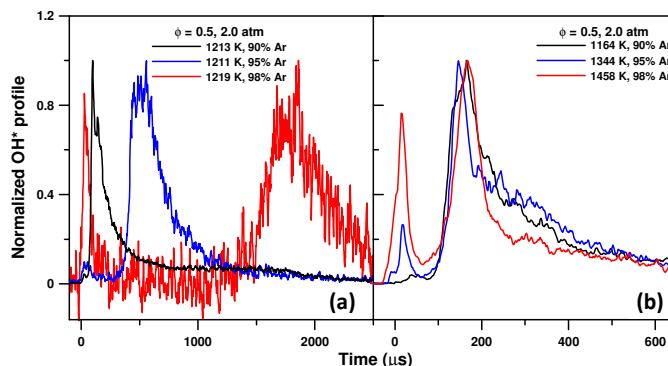


Figure 5: Evolution of the OH* profile with time for (a) a similar temperature and (b) a similar ignition delay time as a function of the dilution level in Ar for mixtures around 2 atm and for an equivalence ratio of 0.5.

5 References

- [1] Cracknell RF et al. (2009). The chemical origin of octane sensitivity in gasoline fuels containing nitroalkanes. *Combust. Flame* 156: 1046.
- [2] Kalghatgi GT. (2005). Auto-Ignition Quality of Practical Fuels and Implications for Fuel Requirements of Future SI and HCCI Engines. SAE Technical Paper 2005-01-0239.
- [3] Brequigny P. et al. (2015). Laminar burning velocities of premixed nitromethane/air flames: An experimental and kinetic modeling study. *Proceed. Combust. Instit.* 35: 703.
- [4] Boyer E, Kuo K. (2007). Modeling of nitromethane flame structure and burning behavior. *Proceed. Combust. Instit.* 31: 2045.
- [5] McCown III KW, Petersen EL. (2014). Effects of nano-scale additives on the linear burning rate of nitromethane. *Combust. Flame* 161: 1935.
- [6] Makovsky A, Gruenwald TB. (1959). The thermal decomposition of nitromethane under high pressure. *Trans. Faraday Soc.* 55: 952.
- [7] Zhang YX, Bauer SH. (1997). Modeling the Decomposition of Nitromethane, Induced by Shock Heating. *J Phys Chem* 101: 8717.
- [8] Glarborg P et al. (1999). Nitromethane dissociation: Implications for the CH₃+NO₂ reaction. *Int. J. Chem. Kinet.* 31: 591.
- [9] Tian Z, et al. (2009). An experimental and kinetic modeling study of a premixed nitromethane flame at low pressure. *Proceed. Combust. Instit.* 32: 311.
- [10] Zhang K et al. (2011). An experimental and kinetic modeling study of premixed nitromethane flames at low pressure. *Proceed. Combust. Instit.* 33: 407.
- [11] Kang JG et al. (1991). Ignition delay times of nitromethane/oxygen/argon mixtures behind reflected shock. *Combust. Flame* 85: 275.
- [12] Aul CJ et al. (2013). Ignition and kinetic modeling of methane and ethane fuel blends with oxygen: A design of experiments approach. *Combust. Flame* 160: 1153.